

## Dependence of Effective Molarity on Linker Length for an Intramolecular Protein–Ligand System

Vijay M. Krishnamurthy, Vincent Semetey, Paul J. Bracher, Nan Shen, and George M. Whitesides\*

*Contribution from the Department of Chemistry and Chemical Biology, Harvard University, 12 Oxford Street, Cambridge, Massachusetts 02138*

Received September 20, 2006; E-mail: gwhitesides@gmwhgroup.harvard.edu

**Abstract:** This paper reports dissociation constants and “effective molarities” ( $M_{\text{eff}}$ ) for the intramolecular binding of a ligand covalently attached to the surface of a protein by oligo(ethylene glycol) ( $\text{EG}_n$ ) linkers of different lengths ( $n = 0, 2, 5, 10,$  and  $20$ ) and compares these experimental values with theoretical estimates from polymer theory. As expected, the value of  $M_{\text{eff}}$  is lowest when the linker is too short ( $n = 0$ ) to allow the ligand to bind noncovalently at the active site of the protein without strain, is highest when the linker is the optimal length ( $n = 2$ ) to allow such binding to occur, and decreases monotonically as the length increases past this optimal value (but only by a factor of  $\sim 8$  from  $n = 2$  to  $n = 20$ ). These experimental results are not compatible with a model in which the single bonds of the linker are *completely* restricted when the ligand has bound noncovalently to the active site of the protein, but they are quantitatively compatible with a model that treats the linker as a random-coil polymer. Calorimetry revealed that enthalpic interactions between the linker and the protein are not important in determining the thermodynamics of the system. Taken together, these results suggest that the manifestation of the linker in the thermodynamics of binding is exclusively entropic. The values of  $M_{\text{eff}}$  are, theoretically, intrinsic properties of the  $\text{EG}_n$  linkers and can be used to predict the avidities of multivalent ligands with these linkers for multivalent proteins. The weak dependence of  $M_{\text{eff}}$  on linker length suggests that multivalent ligands containing flexible linkers that are longer than the spacing between the binding sites of a multivalent protein will be effective in binding, and that the use of flexible linkers with lengths somewhat greater than the optimal distance between binding sites is a justifiable strategy for the design of multivalent ligands.

### Introduction

The primary motivation for this paper was to determine the influence of the “linker”—the structural element that connects the binding moieties in a multivalent ligand—on the binding of a multivalent ligand to a multivalent protein (Figure 1E). As our model system, we adopted a ligand covalently tethered to the surface of a protein by oligo(ethylene glycol) linkers ( $\text{EG}_n$ ) (Figure 1D), because this design allows us to interrogate the system without complications from separate binding events of the two ends of the ligand, complications that do arise when both ends are free. We report dissociation constants (and effective molarities, see below) for the intramolecular binding of the tethered ligand to the active site of the protein as a function of the linker length ( $n$ ) and discuss the data in the context of four possible models (Figure 2). We find that only one of these models (Figure 2B) is consistent with the following results: the linker plays an exclusively entropic role in the thermodynamics of the system, and it has significant conformational mobility even after the ligand is bound at the active site of the protein. The results are quantitatively well-explained by a model that describes the linker as a random-coil polymer (Figure 3); this model is one originally proposed by Lees and co-workers for a related problem and

estimates the probability of intramolecular binding as the probability that the ends of the linker are separated by a distance ( $d$ ) equal to the separation of the sites of covalent attachment and noncovalent binding of the ligand to the protein (Figure 1D).<sup>1</sup>

Effective molarity ( $M_{\text{eff}}$ ) is an empirical term that is commonly used to relate the kinetics and equilibria of intramolecular and intermolecular reactions (both covalent and noncovalent) in chemistry (eq 1).<sup>2,3</sup>  $K_{\text{d}}^{\text{inter}}$ , which has units of concentration (e.g., molarity), is the dissociation constant for an intermolecular reaction (Figure 1A), and  $K_{\text{d}}^{\text{intra}}$ , which is dimensionless, is the dissociation constant for an analogous intramolecular reaction (Figure 1B).  $M_{\text{eff}}$  depends on the length and flexibility of the “linker” between the two reactive groups.<sup>2,3</sup>

$$M_{\text{eff}} = K_{\text{d}}^{\text{inter}}/K_{\text{d}}^{\text{intra}} \quad (1)$$

(1) Gargano, J. M.; Ngo, T.; Kim, J. Y.; Acheson, D. W. K.; Lees, W. J. *J. Am. Chem. Soc.* **2001**, *123*, 12909–12910.

(2) (a) Page, M. I.; Jencks, W. P. *Proc. Natl. Acad. Sci. U.S.A.* **1971**, *68*, 1678–1683. (b) Page, M. I. *Chem. Soc. Rev.* **1973**, *2*, 295–323. (c) Kirby, A. J. In *Advances in Physical Organic Chemistry*; Gold, V., Bethell, D., Eds.; Academic Press: London, 1980; Vol. 17, pp 183–278.

(3) Mandolini, L. In *Advances in Physical Organic Chemistry*; Gold, V., Bethell, D., Eds.; Academic Press: London, 1986; Vol. 22, pp 1–111.

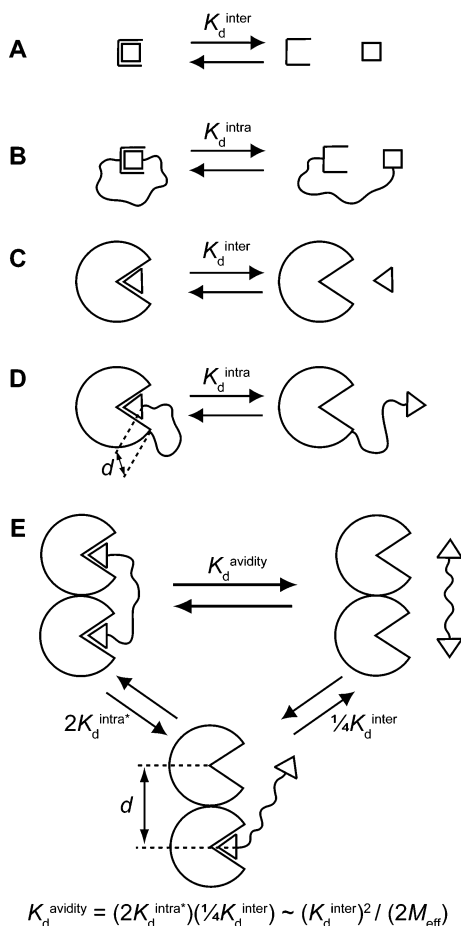


**Figure 1.** (A) A monovalent binding event between a receptor and ligand is characterized by a dissociation constant ( $K_d^{\text{inter}}$ ) with units of concentration (M). (B) When the ligand is tethered to the receptor, the dissociation constant ( $K_d^{\text{intra}}$ ) is now dimensionless and is related to  $K_d^{\text{inter}}$  by the effective molarity,  $M_{\text{eff}}$  (eq 1). (C) Analogous to (A) for a binding event between a protein and ligand. (D) Analogous to (B) for an intramolecular protein–ligand binding event. In this case, however, the distance ( $d$ ) between the two ends of the linker in the bound state is nonzero (unlike the case in (B)). (E) Dissociation of a bivalent ligand from a bivalent receptor. This process can be conceptualized as occurring in two steps: the first step (with dissociation constant  $2K_d^{\text{intra}^*}$ ) is intramolecular, and the second step (with dissociation constant  $1/4 K_d^{\text{inter}}$ ) is intermolecular. The equation given provides a means of estimating  $M_{\text{eff}}$  from the observed dissociation constant ( $K_d^{\text{avidity}}$ ) and the intermolecular dissociation constant ( $K_d^{\text{inter}}$ ) by assuming that the dissociation constant for the first step is equivalent to the product of a statistical factor of 2 and  $K_d^{\text{intra}}$  (defined in (D)); i.e., this procedure assumes that  $K_d^{\text{intra}^*} = K_d^{\text{intra}}$ . This assumption is often quite poor because of complications arising from the influence of binding at one site on binding at the other site (e.g., cooperativity between binding sites, enthalpy/entropy compensation).<sup>4</sup>

Effective concentration ( $C_{\text{eff}}$ , units of concentration) is a theoretical parameter that allows the rate and/or equilibrium for ring closure for intramolecular reactions (Figure 1B) to be estimated by assuming that the linker between the two reactive groups behaves as a random-coil polymer (Figure 3A).<sup>3–7</sup> It is essentially the probability that the two reactive groups (the two ends of the polymer) will be within an infinitesimal distance of

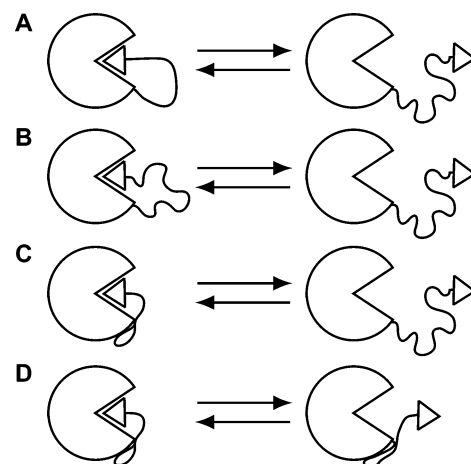


**Figure 2.** Possible models to explain the binding of a ligand, covalently attached to the surface of a protein by the “linker,” to the active site of that protein. When the ligand is bound at the active site, the linker (A) has low conformational mobility (i.e., free rotations of the bonds of the linker are significantly restricted), (B) has significant conformational mobility, or (C,D) makes stabilizing contacts with the surface of the protein. In (D), the linker makes contacts with the surface of the protein even when the ligand is not bound at the active site.

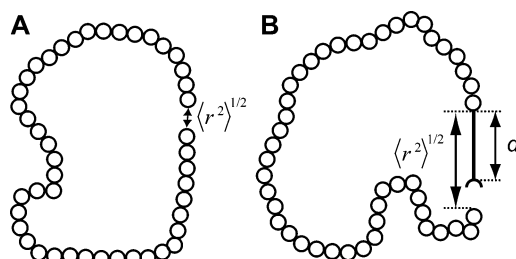


**Figure 3.** Random-coil polymer with the number ( $n$ ) of repeat units (represented as open circles) equal to 45. (A) The polymer forms a closed loop: the distance ( $\langle r^2 \rangle^{1/2}$ ) between the ends of the polymer is near zero. (B) The polymer bears a physical pole of length  $d$  attached at one end. The distance ( $\langle r^2 \rangle^{1/2}$ ) between the ends of the polymer is close to this defined distance ( $d$ ).

one another (eq 2);  $N_A$  is Avogadro’s number and  $\langle r^2 \rangle^{1/2}$  is the root-mean-squared distance (in decimeters) between the ends of the polymer.

$$C_{\text{eff}} = \frac{1}{N_A \langle r^2 \rangle^{1/2}{}^3} \left( \frac{3}{2\pi} \right)^{3/2} \quad (2)$$

The parameter  $\langle r^2 \rangle^{1/2}$  can be estimated from polymer chemistry assuming a three-dimensional random flight (eq 3), where  $n$  is the number of segments in the chain and  $C$  is proportional to the distance ( $l$ ) between two segments of the chain (this value is equal to the bond length for a freely jointed polymer) and is characteristic of a given chain structure.<sup>5,8,9</sup> The proportionality constant  $C/l$  gives a measure of the stiffness of the chain and takes into account effects such as bond angles and rotational barriers; it typically varies from 1.5 for a very flexible chain to 5.5 for a very stiff one.<sup>5,6</sup>

(7) Kramer, R. H.; Karpen, J. W. *Nature* **1998**, *395*, 710–713.

(8) Flory, P. J. *Principles of Polymer Chemistry*; Cornell University Press: Ithaca, NY, 1953.

(9) In order for the theory to apply, the polymer must be long enough to eliminate the possibility of non-ideal effects (e.g., the non-Gaussian nature of short chains, correlations between bond angles of different subunits, transannular steric effects; see refs 5 and 10). Jacobson and Stockmayer have argued that this minimum length is on the order of 15 atoms in the chain, but the exact length depends on the flexibility and structure of the polymer (see ref 10).

(4) Krishnamurthy, V. M.; Estroff, L. A.; Whitesides, G. M. In *Fragment-based Approaches in Drug Discovery*; Jahnke, W., Erlanson, D. A., Eds.; Wiley-VCH: Weinheim, 2006; Vol. 34, pp 11–53.

(5) Jacobson, H.; Stockmayer, W. H. *J. Chem. Phys.* **1950**, *18*, 1600–1606.

(6) Mulder, A.; Auletta, T.; Sartori, A.; Del Ciotto, S.; Casnati, A.; Ungaro, R.; Huskens, J.; Reinhoudt, D. N. *J. Am. Chem. Soc.* **2004**, *126*, 6627–6636.

$$\langle r^2 \rangle^{1/2} = (Cl)l\sqrt{n} = C\sqrt{n} \quad (3)$$

Winnik and Mandolini have reviewed the literature for ring-closing (macrocyclization) reactions in small-molecule systems and concluded that  $C_{\text{eff}}$  and  $M_{\text{eff}}$  are closely correlated for many of these reactions.<sup>3,10</sup>

In many situations (and, in particular, in protein–ligand binding), we are not concerned with the probability that the two ends of the linker are an infinitesimal distance apart. Rather, we require the probability that the two ends are a distance  $d$  apart, where  $d$  is set by the system (Figures 1D,E and 3B). Lees and co-workers derived eq 4 for this case, where  $C_{\text{eff}}(0)$  is  $C_{\text{eff}}$  defined in eq 2.<sup>1</sup> The parameter  $p$  arises because of the presence of the protein: the ligand cannot occupy the same space as the protein, and because it is excluded from this volume, its  $C_{\text{eff}}$  increases (a so-called “excluded volume” effect). Lees and co-workers proposed a value of 2 for this term; this value assumes that the ligand has only a hemisphere of free access when constrained by the protein (Figure 1E), as compared to a sphere when it is free in solution.<sup>1</sup>

$$C_{\text{eff}}(d) = pC_{\text{eff}}(0) \exp\left(-\frac{3}{2\langle r^2 \rangle^{1/2}} d^2\right) \quad (4)$$

We have defined multivalency as multiple interactions (often of the same kind) between two different species.<sup>4,11</sup> Theoretical approaches to multivalency have assumed a stepwise pathway for dissociation, in which the first step is intramolecular (Figure 1E). The value of the dissociation constant ( $2K_{\text{d}}^{\text{intra}}$ ) for this step has been a challenge to estimate theoretically.<sup>4</sup> Without an estimate for this parameter, we cannot *predict* multivalent avidities from the component monovalent affinities (although the work by Lees, Reinhoudt, and others represents a significant advance toward this capability).<sup>1,6,7</sup> The study presented here clarifies and simplifies this problem, because we obtain empirical estimates for the dissociation constants for intramolecular protein–ligand binding that are applicable to the thermodynamics of the intramolecular step in multivalent binding (Figure 1D,E).

We have previously argued that flexible oligomers should not function effectively as linkers in multivalent ligands because of the severe loss in conformational entropy of the linker ( $T\Delta S^\circ \approx RT \ln 3 \approx 0.7 \text{ kcal mol}^{-1}$  per freely rotating single bond of the linker) when it is bound at both ends.<sup>4,11,12</sup> Flexible linkers (e.g., oligo(ethylene glycol)) have, however, been used with success in multivalent ligands.<sup>4,7,11,13</sup> Determining how flexible linkers could work in multivalent ligands, when this simple theoretical model argues that they should not, was a key motivation for this paper.

**Experimental Design.** We selected the combination of human carbonic anhydrase II (HCA, EC 4.2.1.1) and *p*-substituted benzenesulfonamides as our model system, because it is the simplest one that we know for studying protein–ligand interactions: the conserved mode of binding of sulfonamides to HCA has been well-established by X-ray crystallography,

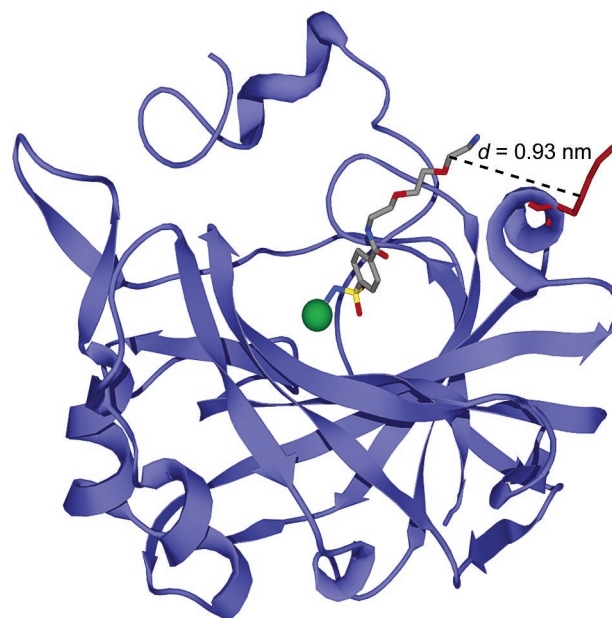


**Figure 4.** Model for the interaction of *p*-H<sub>2</sub>NSO<sub>2</sub>C<sub>6</sub>H<sub>4</sub>CONH(CH<sub>2</sub>CH<sub>2</sub>O)<sub>2</sub>-CH<sub>2</sub>CH<sub>2</sub>NH<sub>3</sub><sup>+</sup> (ArEG<sub>3</sub>NH<sub>3</sub><sup>+</sup>) with HCA based on the deposited X-ray crystallographic coordinates (PDB code 1CNX).<sup>21</sup> The arylsulfonamide ligand is rendered as a ball-and-stick model in CPK color scheme. HCA is depicted as a light blue ribbon diagram, with the catalytically essential Zn<sup>2+</sup> cofactor shown as a green sphere. Lys-133 of HCA II is represented as a red ball-and-stick model. The distance ( $d$ ) between the last glycol unit of the ligand and the  $\gamma$ -CH<sub>2</sub> group of Lys-133 (corresponding to the thiol in the Lys→Cys HCA\*\* mutant) is indicated by the dashed line.

there are a number of well-characterized assays to use in following binding, and there are a number of commercially available, high-affinity arylsulfonamides to use for competition experiments.<sup>14–17</sup> Further, HCA is easy to overexpress in, and purify from, *Escherichia coli* culture in high yield; this ease allows the generation of HCA mutants with chemical “handles” (i.e., reactive sites) to which to couple the ligands.<sup>18–20</sup>

An examination of crystal structures of HCA complexed with *p*-substituted benzenesulfonamides containing oligo(ethylene glycol) linkers (PDB codes 1CNY, 1CNX, and 1CNW)<sup>21</sup> established that Lys-133 was spatially close to the terminus of the ligand but outside of the conical cleft of the enzyme (Figure 4). Mutating this residue to Cys would generate a chemical handle for thiol-selective coupling.<sup>18,20</sup> HCA has an endogenous Cys at position 206. In order to preclude side reaction at this site, we mutated it to Ser to generate a double mutant (Cys-206→Ser, Lys-133→Cys), which we refer to as HCA\*\* in the remainder of this paper. Krebs and Fierke demonstrated that the C206S mutant of HCA is active,<sup>22</sup> and Mårtensson et al. determined that this mutant is as stable as wild-type HCA.<sup>20</sup>

(10) Winnik, M. A. *Chem. Rev.* **1981**, *81*, 491–524.

(11) Mammen, M.; Choi, S.-K.; Whitesides, G. M. *Angew. Chem., Int. Ed.* **1998**, *37*, 2755–2794.

(12) Mammen, M.; Shakhnovich, E. I.; Whitesides, G. M. *J. Org. Chem.* **1998**, *63*, 3168–3175.

(13) Choi, S.-K. *Synthetic Multivalent Molecules: Concepts and Biomedical Applications*; John Wiley & Sons, Inc.: Hoboken, NJ, 2004.

(14) (a) Krishnamurthy, V. M.; Kaufman, G. K.; Urbach, A. R.; Gitlin, I.; Gudiksen, K. L.; Weibel, D. B.; Whitesides, G. M., submitted. (b) Christianson, D. W.; Fierke, C. A. *Acc. Chem. Res.* **1996**, *29*, 331–339.

(15) (a) Supuran, C. T.; Scozzafava, A.; Casini, A. *Med. Res. Rev.* **2003**, *23*, 146–189. (b) Supuran, C. T.; Scozzafava, A.; Conway, J. In *Carbonic Anhydrase: Its Inhibitors and Activators*; Supuran, C. T., Scozzafava, A., Conway, J., Eds.; CRC Press: Boca Raton, FL, 2004; Vol. 1, pp 67–147.

(16) Chen, R. F.; Kernohan, J. C. *J. Biol. Chem.* **1967**, *242*, 5813–5823.

(17) Kernohan, J. C. *Biochem. J.* **1970**, *120*, 26P.

(18) Burton, R. E.; Hunt, J. A.; Fierke, C. A.; Oas, T. G. *Protein Sci.* **2000**, *9*, 776–785.

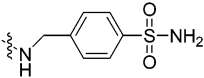
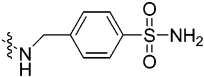
(19) Khalifah, R. G.; Strader, D. J.; Bryant, S. H.; Gibson, S. M. *Biochemistry* **1977**, *16*, 2241–2247.

(20) Mårtensson, L.-G.; Jonsson, B.-H.; Freskgård, P.-O.; Kihlgren, A.; Svensson, M.; Carlsson, U. *Biochemistry* **1993**, *32*, 224–231.

(21) Borjick, P. A.; Christianson, D. W.; Kingery-Wood, J.; Whitesides, G. M. *J. Med. Chem.* **1995**, *38*, 2286–2291.

(22) Krebs, J. F.; Fierke, C. A. *J. Biol. Chem.* **1993**, *269*, 948–954.

**Table 1.** Chemical Labels and Modified HCA\*\* Proteins Used in This Study

Name	R	R'
Pyr-SSEG <sub>n</sub> SA		
HCA**-SSEG <sub>n</sub> SA	HCA**	
Pyr-SSEG <sub>n</sub> CONH <sub>2</sub>		NH <sub>2</sub>
HCA**-SSEG <sub>n</sub> CONH <sub>2</sub>	HCA**	NH <sub>2</sub>

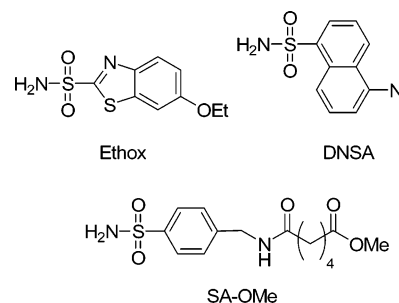
We decided to use *p*-substituted benzenesulfonamides with a conserved alkyl chain (*p*-H<sub>2</sub>NSO<sub>2</sub>C<sub>6</sub>H<sub>4</sub>CH<sub>2</sub>NHCO(CH<sub>2</sub>)<sub>4</sub>-CO-) as our model ligands because benzenesulfonamides bind CA in an invariant orientation, and the alkyl chain should saturate the hydrophobic surface of the conical cleft of CA and orient the linker into solution.<sup>14,21,23–25</sup> We selected oligo(ethylene glycol) (EG<sub>n</sub>) as the linker to tether the ligand to HCA\*\* because it is one of the most common linkers in multivalent ligands.<sup>4,11,13</sup> We wanted to understand how these flexible oligomers could be effective as linkers in multivalent ligands. Oligo(ethylene glycol) has been shown to be resistant to the nonspecific adsorption of proteins when displayed on surfaces;<sup>26</sup> this property should minimize complications from nonspecific adsorption of the linker to the surface of the protein (Figure 2C,D).

We chose thiolate–disulfide interchange as a means of coupling the ligands to HCA\*\* because this reaction is completely selective for thiols (vs the various other chemical functionalities in proteins).<sup>27</sup>

## Results and Discussion

**Synthesis of Benzenesulfonamides Containing Activated Disulfides for Covalent Tethering to HCA\*\*.** We synthesized disulfide-activated *p*-substituted benzenesulfonamides with oligo(ethylene glycol) linkers of different lengths (Pyr-SSEG<sub>n</sub>SA; *n* = 0, 2, 5, 10, and 20; Table 1) using conventional amide-bond coupling reactions (see Supporting Experimental Proce-

dures, Supporting Information for details). We used ligands containing disulfides activated with 2-pyridylthiol because the aromatic thiol is an excellent leaving group; thus, incubating the activated disulfide with HCA\*\* should generate only the desired products (HCA\*\*·SSEG<sub>n</sub>SA).<sup>28</sup> We also synthesized two control molecules (Pyr-SSEG<sub>n</sub>CONH<sub>2</sub> and SA-OMe) for our studies.



**Design and Purification of HCA II with a Surface-Accessible Cysteine Residue.** We generated a vector encoding HCA\*\* by conventional site-directed mutagenesis of the plasmid encoding the C206S mutant of HCA (pC206S) and inserted this mutated vector into the backbone of the plasmid encoding wild-type HCA (pACA; both pC206S and pACA were kind gifts of Prof. Carol Fierke, University of Michigan).<sup>22,29</sup> We overexpressed HCA\*\* in *E. coli* (BL21(DE3)) as described by Fierke and co-workers<sup>18</sup> and purified it as described by Khalifah et al.<sup>19</sup> We confirmed the purity of the enzyme by SDS–PAGE and its activity (~100%) by measuring the amount of protein that could bind ethoxzolamide (Ethox), a specific inhibitor of CA (Figure S.1, Supporting Information).<sup>17</sup>

**Synthesis of Modified HCA\*\* Proteins and Characterization of Conjugates.** We treated HCA\*\* with ~5 equiv of one of five disulfide-activated ligands (Pyr-SSEG<sub>n</sub>SA, *n* = 0, 2, 5, 10, and 20) in Tris–sulfate buffer, pH 8.0, and purified the conjugated proteins (HCA\*\*·SSEG<sub>n</sub>SA, *n* = 0, 2, 5, 10, and 20) by exhaustive dialysis. We also synthesized two control proteins (HCA\*\*·SSEG<sub>2</sub>CONH<sub>2</sub> and HCA\*\*·SCH<sub>2</sub>CO<sub>2</sub><sup>−</sup>) by allowing HCA\*\* to react with ~10 equiv of Pyr-SSEG<sub>2</sub>CONH<sub>2</sub> or iodoacetate (see the Experimental Section for details). The use of HCA\*\*·SSEG<sub>2</sub>CONH<sub>2</sub> established the influence of the linker minus the benzenesulfonamide moiety on binding. We used HCA\*\*·SCH<sub>2</sub>CO<sub>2</sub><sup>−</sup> for control studies (see below).

We characterized all of the modified proteins by ESI-MS and, in all cases, observed peaks corresponding to the combined masses of the protein and the reacted ligand (Table S.1, Supporting Information). We examined the HCA\*\*·SSEG<sub>n</sub>SA proteins by size-exclusion high-performance liquid chromatography (SE-HPLC) in order to determine whether a noncovalent dimer was present in any of the samples (Figure S.2, Supporting Information). For HCA\*\*·SSEG<sub>n</sub>SA with *n* = 2, 5, 10, and 20, we saw no evidence for a dimer at a concentration of protein of 20 μM. For HCA\*\*·SSEG<sub>0</sub>SA (i.e., *n* = 0), we observed a peak (~14% of total protein) corresponding in size to a dimer; this peak quantitatively dissociated in the presence of a large excess of Ethox (a high-affinity arylsulfonamide; see next

- (23) (a) Gao, J.; Qiao, S.; Whitesides, G. M. *J. Med. Chem.* **1995**, *38*, 2292–2301. (b) King, R. W.; Burgen, A. S. V. *Proc. R. Soc. London B* **1976**, *193*, 107–125. (c) Cappalunga Bunn, A. M.; Alexander, R. S.; Christianson, D. W. *J. Am. Chem. Soc.* **1994**, *116*, 5063–5068.
- (24) Jain, A.; Huang, S. G.; Whitesides, G. M. *J. Am. Chem. Soc.* **1994**, *116*, 5057–5062.
- (25) Jain, A.; Whitesides, G. M.; Alexander, R. S.; Christianson, D. W. *J. Med. Chem.* **1994**, *37*, 2100–2105.
- (26) (a) Prime, K. L.; Whitesides, G. M. *Science* **1991**, *252*, 1164–1167. (b) Prime, K. L.; Whitesides, G. M. *J. Am. Chem. Soc.* **1993**, *115*, 10714–10721. (c) Mrksich, M.; Whitesides, G. M. In *Poly(ethylene Glycol): Chemistry and Biological Applications*; 1st ed.; Harris, J. M., Zalipsky, S., Eds.; American Chemical Society: Washington, DC, 1997; Vol. 680, pp 361–373.
- (27) (a) Gilbert, H. F. In *Advances in Enzymology and Related Areas of Molecular Biology*; Meister, A., Ed.; Wiley: New York, 1990; Vol. 63, pp 69–172. (b) Lees, W. J.; Whitesides, G. M. *J. Org. Chem.* **1993**, *58*, 642–647. (c) Erlanson, D. A.; Wells, J. A.; Braisted, A. C. *Annu. Rev. Biophys. Biomol. Struct.* **2004**, *33*, 199–223. (d) Erlanson, D. A.; Braisted, A. C.; Raphael, D. R.; Randal, M.; Stroud, R. M.; Gordon, E. M.; Wells, J. A. *Proc. Natl. Acad. Sci. U.S.A.* **2000**, *97*, 9367–9372. (e) Erlanson, D. A.; Hansen, S. K. *Curr. Opin. Chem. Biol.* **2004**, *8*, 399–406.

- (28) Carlsson, J.; Drevin, H.; Axén, R. *Biochem. J.* **1978**, *173*, 723–737.
- (29) Nair, S. K.; Calderone, T. L.; Christianson, D. W.; Fierke, C. A. *J. Biol. Chem.* **1991**, *266*, 17320–17325.
- (30) Krishnamurthy, V. M.; Bohall, B. R.; Semetey, V.; Whitesides, G. M. *J. Am. Chem. Soc.* **2006**, *128*, 5802–5812.

**Table 2.** Measured and Calculated Enthalpy and Entropy Values for Intermolecular and Intramolecular Binding of Sulfonamides to Modified and Unmodified HCA\*\* Proteins

protein	ligand	$K_d \times 10^6$	$\Delta G^\circ$ , kcal mol <sup>-1</sup>	$\Delta H^\circ$ , kcal mol <sup>-1</sup>	$-T\Delta S^\circ$ , kcal mol <sup>-1</sup>
HCA**	DNSA	$0.30 \pm 0.014^{a,b,c}$	$-8.90 \pm 0.15$		
HCA**-SSEG <sub>2</sub> CONH <sub>2</sub>	DNSA	$0.26 \pm 0.008^{a,b,c}$	$-8.98 \pm 0.10$		
HCA**-SCH <sub>2</sub> CO <sub>2</sub> <sup>-</sup>	DNSA	$0.23 \pm 0.007^{a,b,c}$	$-9.05 \pm 0.10$		
	Ethox	$0.0002 \pm 0.00004^{a,b,d}$	$-13.2 \pm 0.6$	$-17.7 \pm 0.4^{e,f}$	$+4.5 \pm 0.7$
	SA-OMe	$0.51 \pm 0.018^{a,b}$	$-8.58 \pm 0.11$		
	SA-OMe	$0.55 \pm 0.03^{a,e}$	$-8.54 \pm 0.16$	$-6.10 \pm 0.12^{e,f}$	$-2.4 \pm 0.2$
HCA**-SSEG <sub>10</sub> SA	Ethox	$6.1 \pm 0.01^{a,e,g}$	$-7.12 \pm 0.08$	$-11.0 \pm 0.6^{e,f}$	$+3.9 \pm 0.6$
	intra <sup>h</sup>	$33 \pm 7^i$	$-6.1 \pm 0.6$	$-6.7 \pm 0.7^{e,f}$	$+0.6 \pm 0.9$

<sup>a</sup> Units of M. <sup>b</sup> Measured by fluorescence either directly or through competition with DNSA.<sup>16,17,24,25</sup> Uncertainties are 95% confidence intervals from curve-fitting. <sup>c</sup> Compare to literature value of  $0.3 \mu\text{M}$  for the binding of DNSA to a Cys-206→Ser mutant of HCA.<sup>22</sup> <sup>d</sup> Compare to literature value of  $0.2 \text{ nM}$  for the binding of Ethox to bovine carbonic anhydrase II.<sup>17</sup> <sup>e</sup> Measured by calorimetry. <sup>f</sup> Uncertainties were assumed to be due primarily to errors in the quantitation of titrant.<sup>30</sup> An uncertainty of 2% of  $\Delta H^\circ$  was taken for the binding to HCA\*\*-SCH<sub>2</sub>CO<sub>2</sub><sup>-</sup> and 5% of  $\Delta H^\circ$  for the binding to HCA\*\*-SSEG<sub>10</sub>SA. <sup>g</sup> Compare to value from fluorescence of  $2.4 \mu\text{M}$  (Table 3). <sup>h</sup> Thermodynamic parameters are those for the intramolecular equilibrium shown in Figure 1D. <sup>i</sup> Dimensionless.

section) and thus represents a noncovalent dimer that is stable on the time scale of the analysis ( $\sim 25$  min). As a stable, noncovalent dimer represents a minor contaminant for HCA\*\*-SSEG<sub>0</sub>SA and is not present for any of the other HCA\*\*-SSEG<sub>*n*</sub>SA proteins, it should not complicate our analysis of dissociation constants (see next section).

We measured the affinity of a well-characterized fluorescent arylsulfonamide, dansylamide (DNSA), for HCA\*\*, HCA\*\*-SCH<sub>2</sub>CO<sub>2</sub><sup>-</sup>, and HCA\*\*-SSEG<sub>2</sub>CONH<sub>2</sub> (Figure S.3, Supporting Information).<sup>16</sup> The values of  $K_d$  for the three proteins were the same (Table 2); this observation suggests that the EG<sub>*n*</sub> linker itself has no effect on the binding of arylsulfonamides to the modified HCA\*\* proteins and that we can use HCA\*\*-SCH<sub>2</sub>CO<sub>2</sub><sup>-</sup> as a surrogate for HCA\*\* for control studies because it is easier to handle (e.g., there is no need for added reductant and no possibility of dimer formation without the reductant).

In order to determine the purity of the sulfonamide-conjugated proteins (HCA\*\*-SSEG<sub>*n*</sub>SA), we examined the fluorescence of the protein (excitation wavelength = 290 nm, emission wavelength = 460 nm) when treated with  $5 \mu\text{M}$  DNSA; this concentration is  $\sim 16$ -fold greater than the  $K_d$  of DNSA for HCA\*\* (Table 2). The only fluorescent species under these conditions is the HCA\*\*-DNSA complex. We assumed that any fluorescence observed was due to residual, unmodified HCA\*\*, because all of the modified proteins have dissociation constants for DNSA too high to bind it at the concentration of DNSA used in the experiment (see below). We constructed a standard curve for the fluorescence of  $5 \mu\text{M}$  DNSA as a function of the concentration of HCA\*\* and used it to interpolate the concentration of unmodified HCA\*\* remaining in the coupling reactions (Figure S.4, Supporting Information). Using these values and the concentrations of total HCA\*\* protein from UV spectroscopy,<sup>31</sup> we obtained purities of 90–95% for HCA\*\*-SSEG<sub>*n*</sub>SA where  $n = 0, 2, 10,$  and  $20$  and  $\sim 80\%$  for  $n = 5$  (see Supporting Experimental Procedures for details). This amount of contamination will not affect values of dissociation constants for these proteins (see next section).

For calorimetric studies where completely homogeneous protein was required, we purified the sulfonamide-conjugated protein (HCA\*\*-SSEG<sub>10</sub>SA) over a column of benzenesulfonamide-conjugated agarose (see Supporting Experimental Procedures for details). Purities were  $\geq 99\%$  (assessed using the standard curve) after this procedure.

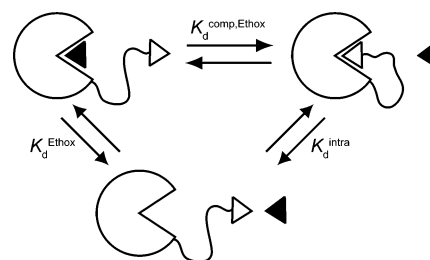


**Figure 5.** Schematic diagram depicting the strategy for the measurement of  $K_d^{\text{intra}}$  for HCA\*\*-SSEG<sub>*n*</sub>SA using the observed dissociation constant ( $K_d^{\text{comp,Ethox}}$ ) for a competing ligand, Ethox (shown as black triangle). For this thermodynamic cycle,  $K_d^{\text{intra}} = K_d^{\text{Ethox}}/K_d^{\text{comp,Ethox}}$  (eq 5).

**Measurement of Dissociation Constants of Ethoxzolamide (Ethox).** Ethox is a high-affinity ligand for CA that quenches  $\sim 70\%$  of the fluorescence of the Trp residues of the enzyme (so-called “intrinsic” protein fluorescence) and thus offers a spectrophotometric method of following binding and determining values of  $K_d$  (Figure S.1B, Supporting Information).<sup>17</sup> We treated HCA\*\*-SSEG<sub>*n*</sub>SA ( $n = 0, 2, 5, 10,$  and  $20$ ) and HCA\*\* (incubated with 2 equiv of SA-OMe) with different concentrations of Ethox and followed the fluorescence of the free, unbound protein (excitation wavelength = 290 nm, emission wavelength = 340 nm) to determine dissociation constants (Figure 5). Figure 6 shows the normalized data and fits to the data assuming a single-site binding model (see Experimental Section). As linker length ( $n$ ) increased,  $K_d^{\text{comp,Ethox}}$  (Figure 5) for HCA\*\*-SSEG<sub>*n*</sub>SA reached a peak when  $n = 2$ , and then decreased. The magnitude of the decrease in  $K_d^{\text{comp,Ethox}}$  was only weakly dependent on  $n$  (only a  $\sim 8$ -fold decrease from  $n = 2$  to  $n = 20$ ; Table 3).

To account for the presence of unmodified HCA\*\* in the HCA\*\*-SSEG<sub>5</sub>SA sample (see previous section), we normalized the fluorescence data (Figure 6) to the intensity observed when [Ethox] =  $40 \text{ nM}$  (this concentration is sufficient to saturate the binding sites of all of the residual unmodified HCA\*\*). Given the high value of  $K_d^{\text{comp,Ethox}}$  ( $5.6 \mu\text{M}$ ) observed for this protein,  $< 1\%$  of the HCA\*\*-SSEG<sub>5</sub>SA in the sample will bind Ethox at this concentration.

The fluorescence of HCA\*\* that had been incubated with  $\sim 2$  equiv of SA-OMe (the ligand that was covalently tethered to HCA\*\* in the modified proteins HCA\*\*-SSEG<sub>*n*</sub>SA) decreased linearly with increasing concentrations of Ethox until a stoichiometric amount of Ethox was present (Figure 6). This result demonstrates that the presence of free, unbound SA-OMe

(31) Nyman, P. O.; Lindskog, S. *Biochim. Biophys. Acta* **1964**, *85*, 141–151.

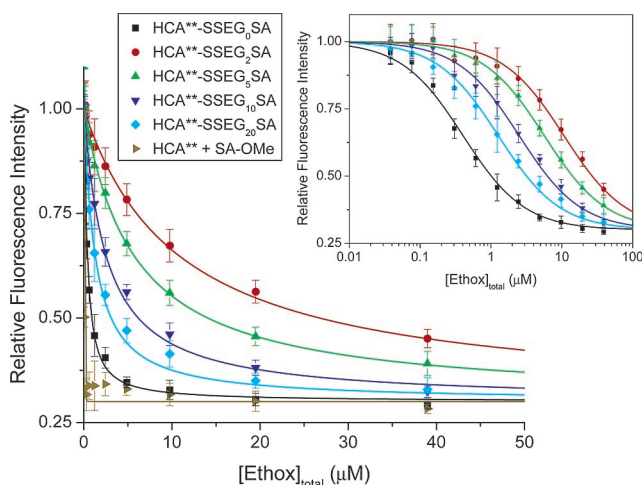


**Figure 6.** Decrease in fluorescence of modified HCA\*\* proteins (HCA\*\*-SSEG<sub>n</sub>SA,  $n = 0, 2, 5, 10, \text{ or } 20$ ) and HCA\*\* (incubated with 2 equiv of SA-OMe) with increasing concentration of ethoxzolamide (Ethox). The intrinsic fluorescence of 200 nM protein in 20 mM sodium phosphate, pH 7.5, at 298 K with different concentrations of the fluorescence quencher Ethox was measured (excitation wavelength = 290 nm, emission wavelength = 340 nm). The data are shown after background subtraction, correction for the inner filter effect, and normalization to a maximum signal of unity (see Experimental Section). The solid curves are fits to the data using the full quadratic equation for binding (eq 7; this equation does not make the assumption that  $[\text{Ethox}]_{\text{free}} \approx [\text{Ethox}]_{\text{total}}$ ), and using a value for the minimum in fluorescence intensity of all samples of 0.3 (Figure S.1B, Supporting Information). Error bars represent the maximum variation of an independent measurement from the mean of four experiments (duplicates from two independent experiments). Inset: The data on a logarithmic scale for the  $x$ -axis. The solid curves are fits to the data using a single-site Langmuir binding model (eq 8), which makes the assumption that  $[\text{Ethox}]_{\text{free}} \approx [\text{Ethox}]_{\text{total}}$ ; this assumption is poor when  $n = 0$  or 20 (see Experimental Section).

**Table 3.** Experimental and Theoretical Values for the Intermolecular and Intramolecular Binding of Sulfonamides to Sulfonamide-Conjugated HCA\*\* Proteins (HCA\*\*-SSEG<sub>n</sub>SA)

$n$	$K_d^{\text{comp,Ethox}} (\mu\text{M})^a$	$K_d^{\text{intra}} \times 10^5{}^b$	$M_{\text{eff}} (\text{mM})^c$
0	$0.31 \pm 0.015$	$66 \pm 14$	$0.8 \pm 0.16$
2	$10 \pm 0.7$	$2.0 \pm 0.4$	$26 \pm 5$
5	$5.6 \pm 0.5$	$3.6 \pm 0.8$	$14 \pm 3$
10	$2.4 \pm 0.17$	$8.3 \pm 1.8$	$6.1 \pm 1.3$
20	$1.2 \pm 0.08$	$17 \pm 4$	$3.1 \pm 0.7$

<sup>a</sup> Observed dissociation constants for the binding of Ethox to HCA\*\*-SSEG<sub>n</sub>SA (Figure 5). Uncertainties are 95% confidence intervals from curve-fitting. <sup>b</sup> Calculated dissociation constants for the binding of the tethered ligand to the active site of HCA (Figure 5). Uncertainties were propagated from uncertainties in  $K_d^{\text{comp,Ethox}}$  and  $K_d^{\text{Ethox}}$  (see Table 2). <sup>c</sup> Calculated using eq 1. Uncertainties were propagated from uncertainties in  $K_d^{\text{intra}}$  and  $K_d^{\text{inter}}$  (see Table 2).

could not explain the observation that the affinity of Ethox is much lower for HCA\*\*-SSEG<sub>n</sub>SA than for HCA\*\*, and that the value of  $K_d^{\text{Ethox}}$  (Figure 5) for HCA\*\* is too low to be determined *directly* by this method (i.e., the value of  $K_d^{\text{Ethox}}$  for HCA\*\* is much lower than the concentration of protein, ~200 nM, required for a detectable signal from intrinsic fluorescence).

To determine the value of  $K_d^{\text{Ethox}}$ , we allowed Ethox and DNSA (5  $\mu\text{M}$ ) to compete for the active site of HCA\*\*-SCH<sub>2</sub>-CO<sub>2</sub><sup>-</sup> and measured the decrease in fluorescence of the HCA\*\*-SCH<sub>2</sub>-CO<sub>2</sub><sup>-</sup>-DNSA complex (excitation wavelength = 290 nm, emission wavelength = 460 nm) with increasing concentration of Ethox (Figure S.5, Supporting Information; Table 2).<sup>16,24,25</sup> The value we obtained ( $K_d^{\text{Ethox}} = 0.2$  nM) was in good agreement with one from the literature (Table 2).<sup>17</sup> We used

the same competition experiment with DNSA to determine the value of the dissociation constant of SA-OMe ( $K_d^{\text{inter}} = 0.51$   $\mu\text{M}$ ; Figure 1C and eq 1) for HCA\*\*-SCH<sub>2</sub>-CO<sub>2</sub><sup>-</sup> (Figure S.5, Supporting Information; Table 2).

**Measurement of  $K_d^{\text{intra}}$  and Calculation of  $M_{\text{eff}}$ .** Equation 5 gives the dissociation constant ( $K_d^{\text{intra}}$ ) for the intramolecular binding of the tethered ligand to the active site of HCA\*\* for HCA\*\*-SSEG<sub>n</sub>SA from a thermodynamic cycle for the binding of Ethox to HCA\*\*-SSEG<sub>n</sub>SA (Figure 5). Values of  $K_d^{\text{comp,Ethox}}$  (for HCA\*\*-SSEG<sub>n</sub>SA) and  $K_d^{\text{Ethox}}$  (for HCA\*\*-SCH<sub>2</sub>-CO<sub>2</sub><sup>-</sup>) were measured as described in the previous section. Table 3 lists the calculated values of  $K_d^{\text{intra}}$ .

$$K_d^{\text{intra}} = K_d^{\text{Ethox}} / K_d^{\text{comp,Ethox}} \quad (5)$$

Table 3 also lists values of  $M_{\text{eff}}$  calculated using eq 1 with values of  $K_d^{\text{intra}}$  and  $K_d^{\text{inter}}$  (the dissociation constant for the binding of SA-OMe to HCA\*\*-SCH<sub>2</sub>-CO<sub>2</sub><sup>-</sup>; see previous section and Figure 1C,D).  $M_{\text{eff}}$  was only weakly dependent on linker length ( $n$ ) when  $n \geq 2$ : it decreased by approximately a factor of 8 between  $n = 2$  and  $n = 20$ . The model shown in Figure 2A anticipates a much greater dependence of  $M_{\text{eff}}$  on  $n$  than that observed: the simplest model, which assumes that each single bond in an EG unit of the linker has three possible conformations before binding and only one after binding, anticipates a >10-fold decrease in  $M_{\text{eff}}$  per EG unit (see Introduction).<sup>4,11,12</sup> This model is inconsistent with the weak dependence of  $M_{\text{eff}}$  on  $n$  observed experimentally and can be eliminated.

**Theoretical Values of  $C_{\text{eff}}$  for Intramolecular Binding of Sulfonamide-Conjugated HCA\*\* (HCA\*\*-SSEG<sub>n</sub>SA).** As mentioned in the section on Experimental Design, the “ligand” in HCA\*\*-SSEG<sub>n</sub>SA consists of the benzenesulfonamide moiety and the alkyl chain that is directly attached to it ( $p\text{-H}_2\text{NSO}_2\text{C}_6\text{H}_4\text{-CH}_2\text{NHCO}(\text{CH}_2)_4\text{CO-}$ ); thus, the linker consists of the EG<sub>n</sub> chain and the remainder of the alkyl chain ( $-\text{NH}(\text{CH}_2\text{CH}_2)_n\text{-CH}_2\text{CH}_2\text{NHCOCH}_2\text{CH}_2\text{S-}$ ). Treating the linker as a copolymer allowed us to estimate a value for  $\langle r^2 \rangle^{1/2}$  from the sum of the contributions from the EG<sub>n</sub> and the non-EG<sub>n</sub> portions of the linker (eq 6).<sup>8</sup> For the EG<sub>n</sub> portion of the linker, we used a literature value of 0.58 nm for the parameter  $C$  in eq 3.<sup>32</sup> We assumed that the non-EG<sub>n</sub> portion of the linker was “alkyl-like” and contributed a constant value of 0.40 nm to the linker length.<sup>33</sup>

$$\langle r^2 \rangle^{1/2} = \sqrt{0.58^2 n + 0.40^2} \quad (6)$$

In order to estimate  $C_{\text{eff}}$  (eq 4), we need a value for the distance ( $d$ ) between the sites of covalent attachment of the ligand to the protein and of the ligand bound at the active site (Figure 1D). There are no reported X-ray crystal structures of complexes of HCA with  $p$ -substituted benzenesulfonamides with alkyl tails, so we examined the crystal structure of a complex of HCA with a  $p$ -substituted benzenesulfonamide having a tri-(ethylene glycol) tail ( $\text{ArEG}_3\text{NH}_3^+$ ; Figure 4). We

(32) Knoll, D.; Hermans, J. *J. Biol. Chem.* **1983**, 258, 5710–5715.

(33) There are a seven single bonds in the non-EG<sub>n</sub> portion of the linker (between the thiol of the linker and the  $-\text{NH}-$  of the carboxamide closest to the alkyl chain of the ligand). Using eq 3 with an estimate for  $l$  of 0.153 nm (the C–C bond length) and assuming an ideal, random-flight polymer ( $Cl = 1$ ) gives an estimate of ~0.4 nm for the value of the non-EG<sub>n</sub> portion of the linker.

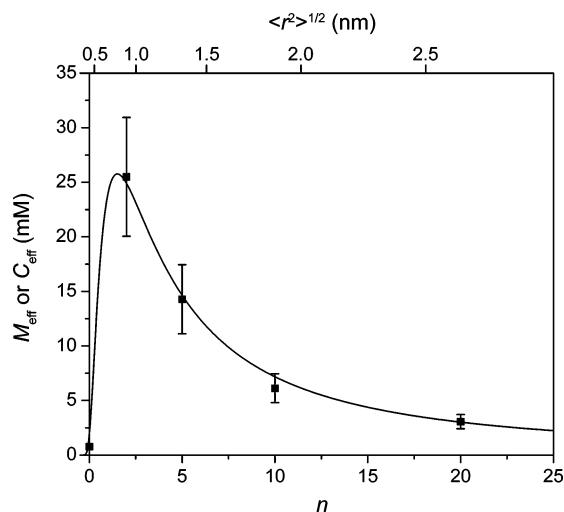


**Figure 7.** Variation of effective concentration ( $C_{\text{eff}}$ ) and effective molarity ( $M_{\text{eff}}$ ) with linker length ( $n$ ); related to the root-mean-squared distance between the ends of the linker  $\langle r^2 \rangle^{1/2}$ , see eq 6) for HCA\*\*SSEG $_n$ SA. The points are empirical values of  $M_{\text{eff}}$  (eq 1) from this study (Table 3). The solid curve is a fit to the data using the definition of  $C_{\text{eff}}$  (eq 4) with estimates of  $\langle r^2 \rangle^{1/2}$  from eq 6. The best fit to the data was obtained with a value for  $d$  (the distance between the site of covalent attachment of the ligand to the protein and the active site of the protein; Figure 4) of  $0.82 \pm 0.03$  nm and a value for  $p$  of  $0.12 \pm 0.009$ .

assumed that the alkyl chain of the ligand in HCA\*\*SSEG $_n$ SA interacts with the same hydrophobic patch of CA and has the same orientation in the active site as the EG $_3$  tail in ArEG $_3$ NH $_3^+$ . From the crystal structure, we estimated a distance of  $\sim 0.9$  nm between the first methylene group of the third glycol unit of ArEG $_3$ NH $_3^+$  (a position that should correspond to the  $-\text{NH}-$  group of the linker in HCA\*\*SSEG $_n$ SA) and the  $\gamma$ -carbon of Lys-133 of HCA (a position that should correspond to the thiol of HCA\*\*) (Figure 4).

Figure 7 shows our experimental values of  $M_{\text{eff}}$  (see previous section) and a fit to the data calculated using eq 4 for  $C_{\text{eff}}$  and eq 6 for  $\langle r^2 \rangle^{1/2}$ . We allowed the values of  $d$  and  $p$  to vary in order to optimize the fit. The value of  $d$  ( $0.82 \pm 0.03$  nm) that gave the best least-squares fit to the data is very close to the value (0.9 nm) that we determined from analyzing the X-ray crystal structure of the HCA-ArEG $_3$ NH $_3^+$  complex (Figure 4). This observation, together with the excellent fit to the experimental data, suggests that the theoretical model based on polymer theory successfully (if unexpectedly) rationalizes the dependence of the intramolecular binding of the tethered ligand to the active site of the protein, as a function of the length of the variable part of the linker. Further, because the theory from which  $C_{\text{eff}}$  is derived explicitly ignores enthalpic contributions to ring closure, these observations suggest that entropy is dominant in intramolecular binding (see the next section for further discussion).

The value of  $p$  ( $0.12 \pm 0.009$ ; eq 4) that gave the best fit to the data is significantly lower than the value of 2 proposed by Lees and co-workers for the bivalent protein–ligand complex (Figure 1E).<sup>1</sup> Because the point of attachment of the benzene-sulfonamide ligands to HCA for HCA\*\*SSEG $_n$ SA is at the periphery of the conical cleft (Figures 1D and 4), the ligand will encounter less steric repulsion with the protein (when it is not bound at the active site of CA) than the unbound ligand in the intermediate state in a bivalent protein–ligand complex (Figure 1E). This effect can decrease the value of  $p$  to no less

than unity—the unbound ligand has a full sphere of volume to explore and is in an environment similar to that of a polymer that is free in solution. At present, we do not have a clear understanding of what effect could contribute the additional 8-fold decrease in  $p$ . We speculate that the geometry of the catalytic cleft of CA ( $\sim 1.5$  nm deep and conical; Figure 4) could result in the polymer being excluded from the cleft because of steric interaction; this excluded volume effect would lower  $p$  (and  $C_{\text{eff}}$ ).

**Calorimetric Investigation To Determine Enthalpy and Entropy of Binding for  $K_d^{\text{intra}}$ .** Our previous work suggested that EG $_n$  tails interacted with a hydrophobic patch in the conical cleft of CA, albeit with no effect on the observed dissociation constants.<sup>21,24</sup> We have recently shown that increasing the length of these tails makes the enthalpy of association of these ligands with CA more favorable and the entropy less favorable in a way that perfectly balances to give no change in values of  $K_d$ .<sup>30</sup> As mentioned in the section on Experimental Design, we designed HCA\*\*SSEG $_n$ SA to include a conserved alkyl chain to saturate this hydrophobic surface in the conical cleft of the enzyme. Thus, we would not anticipate that contacts between the EG $_n$  linker and the surface of HCA could occur (Figure 2C,D).

To test this idea, we used isothermal titration calorimetry (ITC) to dissect the intramolecular dissociation constant ( $K_d^{\text{intra}}$ ; Figures 1D, 2, and 5) for HCA\*\*SSEG $_{10}$ SA into its enthalpic ( $\Delta H^{\circ}_{\text{intra}}$ ) and entropic ( $\Delta S^{\circ}_{\text{intra}}$ ) components. We examined the binding of Ethox to HCA\*\*SSEG $_{10}$ SA (Figure S.6, Supporting Information) and to the control protein HCA\*\*S-CH $_2$ CO $_2^-$  (Figure S.7A, Supporting Information). We calculated  $\Delta H^{\circ}_{\text{intra}}$  and  $\Delta S^{\circ}_{\text{intra}}$  for HCA\*\*SSEG $_{10}$ SA by making use of the thermodynamic cycle shown in Figure 5 (Table 2). The value of  $K_d^{\text{comp, Ethox}}$  that we measured by ITC for the binding of Ethox to HCA\*\*SSEG $_{10}$ SA was in good agreement (a difference of a factor of 2–3) with the one that we measured by fluorescence quenching (Tables 2 and 3).

The value of  $\Delta H^{\circ}_{\text{intra}}$  for HCA\*\*SSEG $_{10}$ SA ( $-6.7 \pm 0.7$  kcal mol $^{-1}$ , Table 2) was the same, within error, as  $\Delta H^{\circ}_{\text{obs}}$  for the binding of SA-OMe (a ligand containing the benzene-sulfonamide moiety and alkyl chain of HCA\*\*SSEG $_{10}$ SA) to HCA\*\*S-CH $_2$ CO $_2^-$  ( $-6.1 \pm 0.12$  kcal mol $^{-1}$ , Table 2 and Figure S.7B, Supporting Information). This result suggests that there is little, if any, interaction of the EG $_n$  linker with the protein: our previous results suggested that any interaction of the EG $_n$  chain with CA should occur with a measurable change in enthalpy.<sup>30</sup> Thus, this result serves to rule out the model shown in Figure 2C.

There remains the possibility that the linker makes stabilizing contacts with the protein whether the ligand is bound or not bound at the active site (Figure 2D), and thus there would be no change in enthalpy for these contacts between the two states. We cannot rigorously rule out this possibility. The fact that a theory from polymer chemistry that is based entirely on entropic terms fits the experimental data very well (Figure 7), however, persuades us to prefer the simpler model shown in Figure 2B.

## Conclusions

This paper reports values of effective molarity ( $M_{\text{eff}}$ ) as a function of the length ( $n$ ) of linkers of oligo(ethylene glycol) for a ligand covalently tethered to a protein (Figure 2). Values

of  $M_{\text{eff}}$  reach a maximum when the linker is the optimal length to allow the ligand to bind to the active site of the protein, and then decrease weakly with increasing linker length (decrease in  $M_{\text{eff}}$  by only a factor of  $\sim 8$  over the range  $n = 2$  to  $n = 20$ ) beyond this value (Figure 7). The experimental data are well-explained by a theoretical, entropic model from polymer chemistry based on the probability that the ends of the linker are separated by the same distance as the sites of covalent attachment and of noncovalent binding of the tethered ligand. Calorimetry revealed that enthalpic contacts of the linker with the protein are not important in this system and that entropy is dominant (Table 2; Figure 2C,D).

Our results suggest that, at least in the case of oligo(ethylene glycol) linkers, contacts of the linker with the surface of the protein (outside of the active site) can be safely ignored. These results are consistent with previous studies that demonstrated that surfaces displaying oligo(ethylene glycol) groups did not adsorb proteins nonspecifically.<sup>26</sup> These results can be reconciled with our previous findings that suggested an interaction of oligo(ethylene glycol) tails with CA: in these previous studies, the tails interacted with a surface of the protein inside the conical cleft of CA.<sup>21,30</sup> This possibility is precluded for the ligands studied here (HCA\*\*<sub>n</sub>-SSEG<sub>n</sub>SA) because they have alkyl chains of sufficient length to saturate this hydrophobic surface.

Most importantly, our results are not consistent with a model in which the linker is *completely* restricted upon association of the ligand with the active site of the protein (when the linker is bound at both ends; Figure 2A). This model requires that  $M_{\text{eff}}$  decrease sharply with the length of the linker ( $> 10$ -fold decrease with each ethylene glycol unit), an expectation that is not met by the experimental results. Our results support a model in which the linker has significant conformational mobility when bound at both ends (Figure 2B).

The values of  $M_{\text{eff}}$  reported here should be intrinsic properties of the oligo(ethylene glycol) linkers themselves. These values can, thus, be used to *predict* the avidities of multivalent ligands containing oligo(ethylene glycol) linkers for a multivalent protein, if the monovalent affinity is known (Figure 1E). Our results suggest, however, that the quantitative accuracy of these predictions is limited by difficulties in estimating the influence of such effects as the “excluded volume” term and the geometric and steric demands of the active site of the protein target on ligand binding (both of which appear in the parameter  $p$  in eq 4).

We did not anticipate the weak dependence of  $M_{\text{eff}}$  on the length of the linker (when it is longer than the optimal length). This *weak* dependence suggests that the most effective strategy for the design of multivalent ligands will connect the ligand moieties by a flexible linker that is significantly longer than the spacing between the multivalent sites of the target protein (Figure 1E). Our results suggest that the penalty in conformational entropy for such a linker in the association of these multivalent ligands with their multivalent proteins will be low (much lower than we previously hypothesized<sup>4,11,12</sup>). Indeed, the results presented here using oligo(ethylene glycol) linkers, which do not interact with the surfaces of proteins, can be seen as a worst-case scenario. Other types of linkers (e.g., alkyl chains) are likely to interact with the surfaces of proteins, and these interactions should effectively “shorten” the linker and

make  $M_{\text{eff}}$  even less sensitive to the length of the linker than in the results presented here (Figure 2C,D).

Finally, ligands with flexible linkers can adopt a number of conformations without steric strain (unlike ligands with rigid linkers); this flexibility should allow the multivalent ligand to sample conformational space to optimize its binding to the multiple binding sites. This sampling of conformational space reduces the possibility of a sterically obstructed fit, a circumstance that can occur readily with rigid linkers that are not perfectly designed.<sup>4</sup>

## Experimental Section

**General Methods.** All chemicals were obtained from Sigma (St. Louis, MO), Aldrich (Milwaukee, WI), or Alfa Aesar (Ward Hill, MA) and used without further purification, unless otherwise noted. DNSA was recrystallized from ethanol prior to use. DNA sequencing was performed by the DNA sequencing facility at the Harvard University Department of Molecular and Cellular Biology. Fluorescence measurements were performed on a Molecular Devices SpectraMax M5 instrument for detection at 340 nm (intrinsic protein fluorescence for Ethox binding assays) and on a Molecular Devices SpectraMax Gemini XS instrument for detection at 460 nm (for DNSA binding assays). Isothermal titration calorimetry was performed using a VP-ITC microcalorimeter from MicroCal (Northampton, MA). Varian Inova spectrometers operating at 400 and 500 MHz (<sup>1</sup>H) were used for NMR experiments. UV-vis spectroscopy was conducted on a Hewlett-Packard 8453 spectrophotometer (Palo Alto, CA). UV spectroscopy was used to quantify HCA\*\* proteins ( $\epsilon_{280} = 54\,000\text{ M}^{-1}\text{ cm}^{-1}$ )<sup>31</sup> and DNSA ( $\epsilon_{326} = 4640\text{ M}^{-1}\text{ cm}^{-1}$ ).<sup>25</sup> Ethox and SA-OMe were quantified by <sup>1</sup>H NMR spectroscopy.<sup>24,25,30,34</sup>

**Preparation of Plasmid Encoding HCA\*\*.** The plasmids encoding wild-type HCA II (pACA) and a Cys-206→Ser mutant of HCA II (pC206S) were gifts from Professor Carol Fierke<sup>22,29</sup> The Lys-133→Cys mutation was introduced into the pC206S plasmid using oligonucleotide site-directed mutagenesis with a Quickchange Mutagenesis Kit (Stratagene) and following the manufacturer's directions. This plasmid was digested with the restriction enzymes *Bam*HI and *Kas*I (New England BioLabs), purified by agarose gel electrophoresis using a Quick Gel extraction kit (Qiagen), and ligated into the pACA backbone, which had been digested with *Bam*HI and *Kas*I, treated with calf intestinal alkaline phosphatase (CIP, from New England BioLabs; to prevent recircularization of the vector without the insert), and purified by gel electrophoresis. The presence of the desired mutation was verified by sequencing the entire HCA II gene using the method of Sanger et al.<sup>35</sup>

**Expression and Purification of HCA\*\*.** BL21(DE3) cells were transformed with the HCA\*\* plasmid and grown as described by Fierke and co-workers (see, for example, ref 18). Cell lysates were prepared as described by Krebs and Fierke,<sup>22</sup> and the HCA\*\* protein was purified using sulfonamide-conjugated agarose (Sigma-Aldrich) as described by Khalifah et al.<sup>19</sup> The purified HCA\*\* protein was stored at  $-80\text{ }^{\circ}\text{C}$  in 50 mM Tris-sulfate buffer, pH 8.0, with 0.2 mM ZnSO<sub>4</sub> and 1 mM DTT (to prevent oxidation of the thiol).

**Preparation of Modified HCA\*\* Proteins.** HCA\*\* was desalted over a NAP-10 column (Amersham) into 50 mM Tris-sulfate buffer, pH 8.0, from which oxygen had been removed by bubbling Ar through it for  $> 1\text{ h}$ . HCA\*\* (50–100  $\mu\text{M}$ ) was treated with 5–10 equiv of the appropriate modifying agent (Pyr-SSEG<sub>n</sub>SA, Pyr-SSEG<sub>2</sub>CONH<sub>2</sub>, or iodoacetate) to generate the desired modified HCA\*\* (HCA\*\*<sub>n</sub>-SSEG<sub>n</sub>SA, HCA\*\*<sub>n</sub>-SSEG<sub>2</sub>CONH<sub>2</sub>, or HCA\*\*<sub>n</sub>-SCH<sub>2</sub>CO<sub>2</sub><sup>-</sup>, respectively). The reaction was allowed to proceed for 1 h at 25  $^{\circ}\text{C}$  and then for  $\sim 18\text{ h}$

- (34) Krishnamurthy, V. M.; Bohall, B. R.; Kim, C.-Y.; Moustakas, D. T.; Christianson, D. W.; Whitesides, G. M. *Chem. Asian J.* **2007**, *2*, 94–105.  
(35) Sanger, F.; Nicklen, S.; Coulson, A. R. *Proc. Natl. Acad. Sci. U.S.A.* **1977**, *74*, 5463–5467.

at 4 °C. The reaction products were purified by exhaustive dialysis and then characterized by electrospray ionization mass spectrometry (ESI-MS) to verify the appearance of a peak corresponding to the combined masses of HCA\*\* and the chemical reactant (see Table S.1, Supporting Information). For the HCA\*\*SSEG<sub>n</sub>SA proteins, contamination by unmodified HCA\*\* was assessed by examining the binding of DNSA (see Supporting Experimental Procedures and Figure S.4, Supporting Information).

**Determination of Dissociation Constants ( $K_d^{\text{comp.Ethox}}$ ) for the Binding of Ethox to HCA\*\*SSEG<sub>n</sub>SA.** To the wells of a black microwell plate were added dilutions of Ethox and then the appropriate HCA\*\* protein (200 nM) in a final volume of 200  $\mu\text{L}$  of 20 mM sodium phosphate, pH 7.5. The plate was allowed to incubate at 25 °C for 2 h, and then its fluorescence was measured with an excitation wavelength of 290 nm and an emission wavelength of 340 nm (with a 325 nm cutoff filter). Wells were read  $\sim$ 50 times. Fluorescence intensities were normalized to the fluorescence intensity of the protein with no added Ethox and then corrected for the inner filter effect<sup>36</sup> by using a control experiment where soybean trypsin inhibitor (a protein with no affinity for sulfonamides)<sup>37</sup> was treated with Ethox. The corrected data were fit to eq 7, where  $[\text{CA}]_{\text{total}}$  is the total concentration of modified HCA\*\* in the assay (200 nM) and  $[\text{Ethox}]_{\text{total}}$  is the total concentration of Ethox (the independent variable). Only the parameter  $K_d^{\text{comp.Ethox}}$  was allowed

$$F = 0.3 + 0.7 \frac{1 - 0.5/([\text{CA}]_{\text{total}}(K_d^{\text{comp.Ethox}} + [\text{CA}]_{\text{total}} + [\text{Ethox}]_{\text{total}} - \sqrt{(K_d^{\text{comp.Ethox}} + [\text{CA}]_{\text{total}} + [\text{Ethox}]_{\text{total}})^2 - 4[\text{CA}]_{\text{total}}[\text{Ethox}]_{\text{total}}))}{K_d^{\text{comp.Ethox}} + [\text{CA}]_{\text{total}} + [\text{Ethox}]_{\text{total}}} \quad (7)$$

to vary to optimize the fit by nonlinear least-squares fitting (Origin), with the other parameters held constant at their known values. Equation 7 assumes that Ethox quenches 70% of the fluorescence of HCA\*\*; this value was determined by examining the fluorescence of HCA\*\* in the presence of Ethox (Figure S.1B, Supporting Information).

The data were also fit to eq 8, which assumes that the concentration of Ethox not bound by CA is equal to the total concentration of Ethox ( $[\text{Ethox}]_{\text{total}}$ ) and gives a sigmoid fit to the data when the concentration of Ethox is plotted on a logarithmic scale. This equality is not true for HCA\*\*SSEG<sub>0</sub>SA and HCA\*\*SSEG<sub>20</sub>SA, because in those cases  $K_d^{\text{comp.Ethox}} \sim [\text{CA}]_{\text{total}}$  (200 nM).

**Isothermal Titration Calorimetry.** In order to determine values of  $\Delta H^\circ$  and  $K_d$ ,  $\sim 6 \mu\text{M}$  HCA\*\*SCH<sub>2</sub>CO<sub>2</sub><sup>-</sup> or  $\sim 60 \mu\text{M}$  HCA\*\*SSEG<sub>10</sub>CA, which had been purified over sulfonamide-conjugated

$$F = 0.3 + 0.7 \frac{K_d^{\text{comp.Ethox}}}{K_d^{\text{comp.Ethox}} + [\text{Ethox}]_{\text{total}}} \quad (8)$$

agarose (see Supporting Experimental Procedures), in 20 mM sodium phosphate buffer, pH 7.5 (with 0.6% DMSO-*d*<sub>6</sub>), was titrated with 120 or 440  $\mu\text{M}$  Ethox, respectively, in the same buffer at 25 °C. HCA\*\*SCH<sub>2</sub>CO<sub>2</sub><sup>-</sup> ( $\sim 6 \mu\text{M}$ ) was also titrated with 120  $\mu\text{M}$  SA-OMe. (See Figures S.6 and S.7, Supporting Information, for details.) After subtraction of background heats, the data were analyzed by a single-site binding model using the Origin software (provided by Microcal) and allowing the values of binding stoichiometry,  $\Delta H^\circ$ , and  $K_d$  to vary to optimize the fit.

**Acknowledgment.** This work was supported by the National Institutes of Health (GM30367). V.M.K. and P.J.B. acknowledge support from NDSEG and NSF pre-doctoral fellowships, respectively. V.S. acknowledges support from La Ligue Contre Le Cancer (France). We thank Prof. Carol Fierke (University of Michigan) for the kind gift of the HCA-encoding plasmids, and Andrea Stoddard (Fierke group, Michigan) for helpful discussions about protein purification. We thank Dr. Julian P. Whitelegge (The Pasarow Mass Spectrometry Laboratory, University of California, Los Angeles) for ESI-MS analysis. We thank Prof. Greg Verdine (Harvard University) for use of the Spectramax M5, and Marie Spong (Verdine group, Harvard) for helpful discussions about molecular biology. We acknowledge the Bauer Center for Genomics Research (Harvard University) for the use of the Spectramax Gemini XS and Perspective Biosystems Voyager-DE PRO for MALDI.

**Supporting Information Available:** Synthetic procedures and characterization, assay protocols, SDS-PAGE and assessment of activity of HCA\*\*, mass spectra and SE-HPLC chromatograms of modified HCA\*\* proteins, fluorescence titration curves for the binding of DNSA to control HCA\*\* proteins, fluorescence calibration plot for determining purity of HCA\*\*SSEG<sub>n</sub>SA proteins, fluorescence titration curves for determination of  $K_d$  of SA-OMe and Ethox to HCA\*\*SCH<sub>2</sub>CO<sub>2</sub><sup>-</sup>, and ITC thermograms for the binding of Ethox and SA-OMe to HCA\*\*SCH<sub>2</sub>CO<sub>2</sub><sup>-</sup> and to HCA\*\*SSEG<sub>10</sub>SA. This material is available free of charge via the Internet at <http://pubs.acs.org>.

JA066780E

(36) Lakowicz, J. R. *Principles of Fluorescence Spectroscopy*, 2nd ed.; Kluwer Academic/Plenum: New York, 1999.

(37) Colton, I. J.; Carbeck, J. D.; Rao, J.; Whitesides, G. M. *Electrophoresis* **1998**, *19*, 367–382.